Applied Physics A (2019) 125:780
https://doi.org/10.1007/s00339-019-3072-0

Applied Physics A
Materials Science & Processing

Room temperature magnetocaloric effect in polycrystalline $La_{0.75}Bi_{0.05}Sr_{0.2}MnO_3$

A. Elghoul[1] · A. Krichene[1] · N. Chniba Boudjada[1,2] · W. Boujelben[1]

Received: 27 August 2019 / Accepted: 4 October 2019 / Published online: 25 October 2019

Abstract
In this work, we have investigated the magnetic and magnetocaloric properties of polycrystalline $La_{0.75}Bi_{0.05}Sr_{0.2}MnO_3$ prepared by sol–gel method. Structural analysis has shown that this compound crystallizes in the rhombohedral structure with $R\bar{3}c$ space group. The magnetic study revealed that our sample exhibits a ferromagnetic–paramagnetic transition at 300 K. A significant magnetocaloric effect in the vicinity of the room temperature was detected for this sample (for only 2T applied field, the maximum of magnetic entropy change $|\Delta S^{Max}| = 1.75$ J/kg K and the relative cooling power RCP = 77.12 J/kg). The obtained results suggest the possibility of using this compound as a magnetic refrigerant.

1 Introduction

Magnetic refrigeration is an ecofriendly cooling technology. It does not use ozone-depleting chemicals, hazardous chemicals, or gases characterized as greenhouse gases like chlorofluorocarbon (CFC) and hydrocarbon (HC). Most modern refrigeration systems and air conditioners still use harmful volatile liquid refrigerants. However, the magnetic refrigeration is rapidly becoming competitive with conventional gas-compression technology because it offers considerable operating cost savings by eliminating the most inefficient part of the refrigerator (compressor). Magnetic refrigeration is based on the magnetocaloric effect (MCE) which can be described as a modification of one sample's temperature due to the adiabatic application of an external magnetic field. Mixed valence manganites generally show important MCE, indicating the possibility of using these compounds as magnetic refrigerants [1–8].

$La_{0.8}Sr_{0.2}MnO_3$ compound is one of the most studied manganites due to its important physical properties, especially a magnetic transition in the vicinity of room temperature [8–16]. Previous studies were carried out on the structural, magnetic and magnetocaloric properties of $La_{0.8}Sr_{0.2}MnO_3$ polycrystalline compound prepared by sol–gel method [8]. This compound crystallizes in the rhombohedral structure with $R\bar{3}c$ space group. The magnetic study has shown a ferromagnetic–paramagnetic transition with increasing temperature at $T_C = 330$ K, this value can even reach 370 K [9–11]. The T_C value for $La_{0.8}Sr_{0.2}MnO_3$ compound seems to be very sensitive to synthesis process as well as substitution [8–16]. In our previous study, we have also investigated the effect induced by partial substitution of lanthanum by other rare earth elements (Ln = Sm, Eu, Gd, Dy and Ho) on the magnetocaloric response of $La_{0.8}Sr_{0.2}MnO_3$. This substitution leads to the decrease of the Curie temperature value near to room temperature which gives birth to possible technological applications [8]. Magnetic interactions for $La_{0.8}Sr_{0.2}MnO_3$ compound were described by the 3D-Ising model [12]. Bismuth is one of the most diamagnetic elements. Despite the fact that La^{3+} and Bi^{3+} ions possess nearly identical values of the ionic radius (~ 1.22 Å) [17], the substitution of La by Bi in manganites generally shows special properties [18–28] due to presence of the $6s^2$ lone pair electrons of Bi^{3+}. Thus, we have tried to add bismuth to $La_{0.8}Sr_{0.2}MnO_3$ in order to bring the magnetic transition to room temperature. In this communication, we report the structural, magnetic and magnetocaloric study of $La_{0.75}Bi_{0.05}Sr_{0.2}MnO_3$ compound.

✉ A. Krichene
akramkri@hotmail.fr

[1] Laboratoire de Physique des Matériaux, Faculté des Sciences de Sfax, Université de Sfax, B.P. 1171, 3000 Sfax, Tunisia

[2] Institut Néel, B.P. 166, 38042 Grenoble Cedex 9, France

2 Experimental techniques

Polycrystalline $La_{0.75}Bi_{0.05}Sr_{0.2}MnO_3$ was synthesized from high purity (99.9%, Sigma-Aldrich) precursors La_2O_3, Bi_2O_3, $SrCO_3$ and MnO_3 using sol–gel method according to the following reactions:

$$0.375La_2O_3 + 0.2SrCO_3 + 0.025Bi_2O_3 + MnO_2 \rightarrow La_{0.75}Bi_{0.05}Sr_{0.2}MnO_3 + 0.2CO_2 + 0.2O_2$$

All precursors were mixed in stoechiometric proportions with diluted nitric acid and the mixture was then heated to 80 °C to eliminate the excess of water. After 3 h, we added ethylene glycol and citric acid to obtain the gel that was dried at 300 °C and then calcinated at 600 °C for 20 h. The obtained powder was ground in an agate mortar for 1 h then pressed into pellets and sintered at 800 °C for 20 h. We have repeat the last cycle (grinding, pelletizing and sintering) at 1000 °C and 1200 °C for 20 h to obtain a single-phase powder. The phase purity of our compound was confirmed by X-ray diffraction (XRD) technique using CuKα radiation. The chemical composition and the morphology of our studied sample were studied using a JEOL 840 A scanning electron microscopy (SEM). The magnetic measurements were carried out using a vibrating sample magnetometer (SQUID VSM from Quantum Design) under different magnetic applied fields up to 7T in the temperature range 5–350 K. The MCE of our sample has been calculated using thermodynamic equations.

3 Results and discussion

3.1 Structural and morphological properties

Figure 1 shows the energy-dispersive X-ray (EDX) of our studied sample. EDX study confirms the presence of La, Bi, Sr, Mn and O elements and the absence of other elements. The inset of Fig. 1 shows the XRD pattern recorded at room temperature for our sample. Using Rietveld refinement, we have found that our sample is single-phased and crystallizes in the rhombohedral structure with $R\bar{3}c$ space group. The bismuth substitution did not induce a structural transition comparing to parent compound $La_{0.8}Sr_{0.2}MnO_3$ [8]. Besides, reliability factors for our refinement are $\chi^2 = 2.82$ and Bragg R-factor = 2.88, which confirms the refinement quality. The

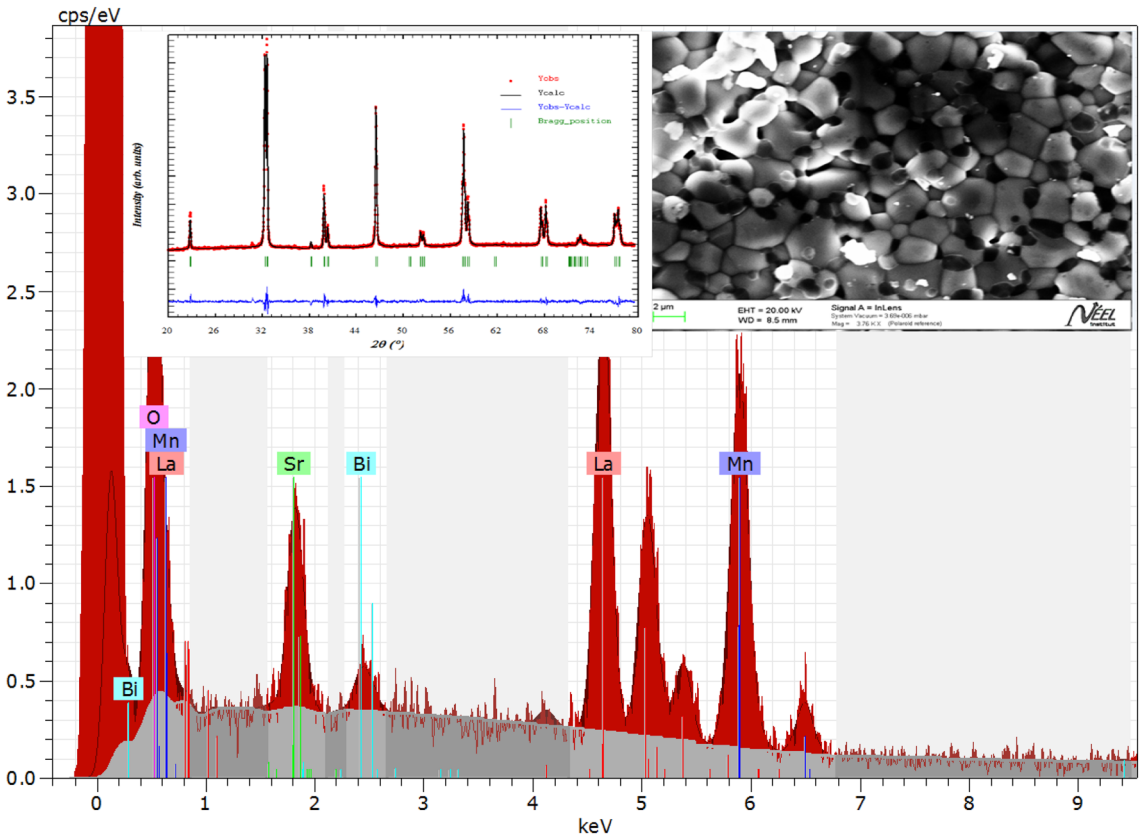

Fig. 1 Energy-dispersive X-ray of $La_{0.75}Bi_{0.05}Sr_{0.2}MnO_3$ compound. The inset shows the scanning electron micrograph and Rietveld refinement for this sample

Table 1 Refinement results for the $La_{0.75}Bi_{0.05}Sr_{0.2}MnO_3$ and $La_{0.8}Sr_{0.2}MnO_3$ [8] samples

Compound	$La_{0.75}Bi_{0.05}Sr_{0.2}MnO_3$	$La_{0.8}Sr_{0.2}MnO_3$ [8]
a (Å)	5.542	5.531
c (Å)	13.413	13.390
V (Å^3)	356.743	354.747
Mn–O (Å)	1.976(4)	1.972(2)
Mn–O–Mn (°)	161.83(4)	162.15(4)
Bragg F-Factor	2.88	3.38
χ^2	2.82	3.44
D_{SC} (nm)	18.5	20
D_{SEM} (nm)	600	551

refinement results were summarized in Table 1. We can notice that the structural parameters are very close to those of parent compound. In fact, since La^{3+} and Bi^{3+} possess similar radii, the substitution did not change neither the average ionic radius at A-site $\langle r_A \rangle$, nor the cationic mismatch σ^2, which gives similar structural parameters. SEM image for our compound is shown in the inset of Fig. 1. In our case, one can observe that the grains possess different sizes with island-like shapes and that the grain boundaries are clearly visible. The micrograph reveals that the surface of our sample is homogeneous. The average grain size is around 0.6 µm, this value is much larger than the one calculated from the width of diffraction peaks using Scherrer relation ($D_{SC} = \frac{K\lambda}{\beta \cos\theta} = 18.50$ nm) because, each grain is composed of several crystallites due to the agglomeration induced by high sintering temperature.

3.2 Magnetic and magnetocaloric properties

Temperature dependence of magnetization for $La_{0.75}Bi_{0.05}Sr_{0.2}MnO_3$ compound (Fig. 2) has been carried out using zero-field cooled (ZFC) and field cooled (FC) protocols under an applied field of 0.05T in the temperature range 5–330 K. In ZFC process, the compound was cooled from 330 to 5 K in the absence of magnetic field and then the magnetization measurement was performed under 0.05T when warming the sample from 5 to 330 K. In FC process, the magnetization measurement was carried out under the same magnetic field while cooling the sample from 330 to 5 K. The $La_{0.75}Bi_{0.05}Sr_{0.2}MnO_3$ compound shows a paramagnetic-ferromagnetic transition with decreasing temperature at Curie temperature T_C equal to 300 K. The bismuth substitution decreases the Curie temperature from 330 K for the parent compound [8] to 300 K. Therefore, our Bi based compound exhibits a magnetic transition at room temperature, which is crucial for technological applications. The decrease of T_C can be ascribed to the weakening of ferromagnetic

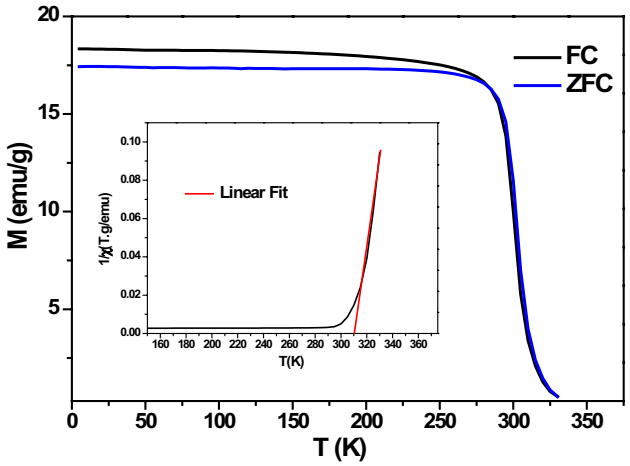

Fig. 2 Temperature dependence of magnetization under an applied magnetic field of 0.05T for $La_{0.75}Bi_{0.05}Sr_{0.2}MnO_3$ sample. The inset shows the temperature dependence of the inverse of paramagnetic susceptibility

interactions induced by the $6s^2$ lone pair electrons of Bi^{3+} ions [18–28]. To study the magnetic interactions in the paramagnetic region, we have represented in the inset of Fig. 2 the temperature dependence of the inverse of paramagnetic susceptibility for our compound. We have noticed that the Curie–Weiss law ($\chi^{-1} = \frac{T-\theta_P}{C_P}$) is well respected in the paramagnetic phase for our sample through the linear shape of χ^{-1} above T_C. Experimental and theoretical effective paramagnetic moments μ_{eff}^{exp} and μ_{eff}^{th} are determined from the following relations:

$$C_P = \frac{N\mu_B^2}{3k_B}\left(\mu_{eff}^{exp}\right)^2 \quad (1)$$

$$\mu_{eff}^{th} = \sqrt{\left(\sum_i y_i \mu_i^2\right)\mu_B^2} \quad (2)$$

where k_B is Boltzmann constant, N is the number of magnetic moment carriers, μ_B is the Bohr magnetron and μ_i is the magnetic moment of the ion i with the fraction y_i. Using relations (1) and (2), we have obtained $\mu_{eff}^{exp} = 6.88\mu_B$ and $\mu_{eff}^{th} = 4.71\mu_B$. It is relevant that the experimental value is larger than the theoretical one indicating the presence of some magnetic ordering just above T_C. We have presented in Fig. 3 the magnetic field dependence of magnetization in the vicinity of T_C for our sample. The $M(H)$ curves indicate that the ground state of our compound is ferromagnetic below T_C. For temperature values well above T_C, the compound is paramagnetic and the magnetization curves become linear. However, it should be noted that just above T_C, the curves do not exhibit the conventional linear behavior, testifying

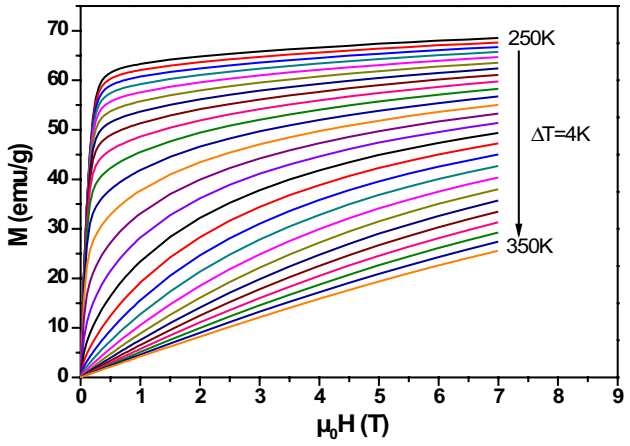

Fig. 3 Magnetic field dependence of magnetization at several values of temperature for $La_{0.75}Bi_{0.05}Sr_{0.2}MnO_3$ sample

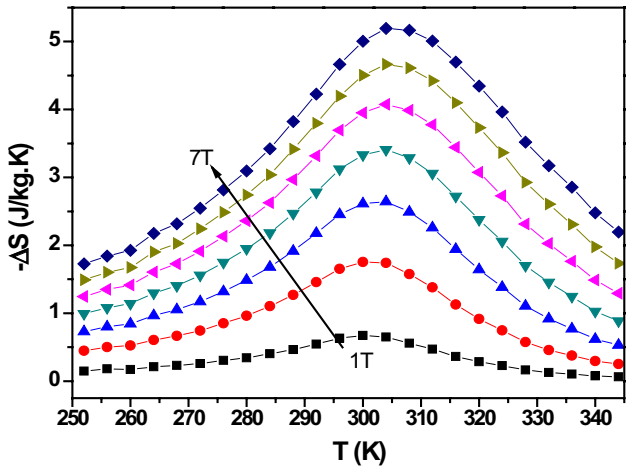

Fig. 4 Evolution of magnetic entropy change as a function of temperature under several values of applied magnetic field for $La_{0.75}Bi_{0.05}Sr_{0.2}MnO_3$ sample

the presence of some ferromagnetic interactions above T_C, which is in agreement with the difference between μ_{eff}^{exp} and μ_{eff}^{th}.

The magnetic entropy change ΔS, was calculated from Maxwell's relation and isothermal magnetization measurements. ΔS can be defined using the following equation [29]:

$$\Delta S(T,H) = \sum_i \frac{M_{i+1}(T_{i+1},H) - M_i(T_i,H)}{T_{i+1} + T_i}\Delta H \quad (3)$$

where M_i and M_{i+1} are the experimental values of magnetization measured at temperatures T_i and T_{i+1}, respectively, under an applied magnetic field H. Figure 4 shows the variation of $(-\Delta S)$ as a function of the temperature for different magnetic field values up to 7T for the $La_{0.75}Bi_{0.05}Sr_{0.2}MnO_3$ compound. All the curves exhibit a peak around T_C, and the maximum value increases with increasing the applied field. We can observe that the values are significant for our sample at the room temperature ($T_C = 300$ K), which suggests the possibility of using this sample in the magnetic refrigeration field. To evaluate the MCE, we can estimate the relative cooling power (RCP) according the following equation:

$$RCP = -\Delta S^{Max} \times \delta T_{FWHM} \quad (4)$$

where δT_{FWHM} is the full width at half maximum of the magnetic entropy change curve. We have regrouped in Table 2 the values of T_C, $-\Delta S^{Max}$, δT_{FWHM} and RCP under 2T and 4T applied magnetic fields for parent compound [8] as well as our Bi substituted compound. We have noticed that the substitution lanthanum by Bi^{3+} ions increases RCP values at the room temperature and enhance the MCE. Thus, our sample can be considered as a good candidate in the field of magnetic refrigeration at the room temperature. It is noteworthy that substitution reduces the maximum of $(-\Delta S)$ compared to the parent compound, which can be explained by the weakening of ferromagnetic interactions induced by Bi^{3+} ions. However, the increase of transition width (δT_{FWHM}) gives significant values of RCP near room temperature. To identify the nature of the magnetic transition in the case of our Bi based specimen, we have tried to get the phenomenological universal curve that can be constructed by normalizing all the ΔS curves ($\Delta S/\Delta S^{Max}$) and rescaling the temperature axis above and below T_C using the following relations [30]:

$$\theta = \begin{cases} -(T - T_C)/(T_{r1} - T_C); & T \le T_C \\ (T - T_C)/(T_{r2} - T_C); & T > T_C \end{cases} \quad (5)$$

where T_{r1} and T_{r2} are the temperatures of the two reference points corresponding to $\Delta S = \Delta S^{Max}/2$. Figure 5 shows that the variation of $\Delta S/\Delta S^{Max}$ as a function of rescaled temperature θ nearly exhibits the same shape for different field values up to 7T. This behavior proves that the magnetic phase transition is of second order for the $La_{0.75}Bi_{0.05}Sr_{0.2}MnO_3$ compound.

Table 2 T_C, ΔS^{Max}, δT_{FWHM}, and RCP values for $La_{0.75}Bi_{0.05}Sr_{0.2}MnO_3$ and $La_{0.8}Sr_{0.2}MnO_3$ [8] samples under 2 T and 4 T applied magnetic fields

Sample	T_C (K)	$-\Delta S^{Max}$ (J/kg K)		δT_{FWHM} (K)		RCP (J/kg)	
		2T	4T	2T	4T	2T	4T
$La_{0.8}Sr_{0.2}MnO_3$ [8]	330	1.99	3.69	34.71	36.60	69.07	135.04
$La_{0.75}Bi_{0.05}Sr_{0.2}MnO_3$	300	1.75	3.41	43.99	52.86	77.12	180.16

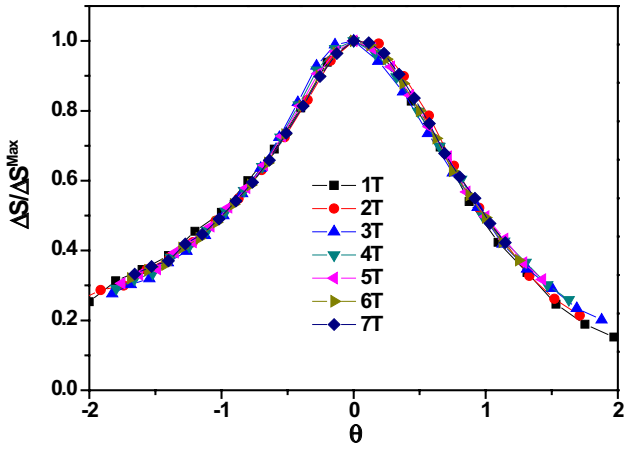

Fig. 5 Normalized entropy change as a function of the rescaled temperature θ for $La_{0.75}Bi_{0.05}Sr_{0.2}MnO_3$ sample

4 Conclusion

$La_{0.75}Bi_{0.05}Sr_{0.2}MnO_3$ bulk manganite, synthesized by sol–gel technique, is characterized by a significant MCE at room temperature. A considerable RCP value was recorded for our compound (77.12 J/kg under an applied magnetic field of 2 T), suggesting the possibility of using this compound for magnetic refrigeration field at room temperature. The $6s^2$ lone pair of Bi ions seems to play a crucial role in the magnetic response of the studied sample.

References

1. A.R. Shelke, K.P. Shinde, N. Patra, S.N. Jha, D. Bhattacharyya, K.C. Chung, Y.P. Lee, D.M. Phase, S.D. Kaushik, N.G. Deshpande, J. Magn. Magn. Mater. **480**, 22 (2019)
2. A. Jerbi, A. Krichene, R. Thaljaoui, W. Boujelben, J. Supercond. Nov. Magn. **29**, 123 (2016)
3. A. Elghoul, A. Krichene, W. Boujelben, J. Phys. Chem. Solids **98**, 263 (2016)
4. M. Bourouina, A. Krichene, N. Chniba Boudjada, W. Boujelben, Ceram. Int. **43**, 12311 (2017)
5. A. Jerbi, R. Thaljaoui, A. Krichene, W. Boujelben, Physica B **442**, 21 (2014)
6. M. Bourouina, A. Krichene, N. Chniba Boudjada, W. Boujelben, J. Alloys Compd. **680**, 67 (2016)
7. A. Jerbi, A. Krichene, N. Chniba Boudjada, W. Boujelben, Physica B **477**, 75 (2015)
8. A. Elghoul, A. Krichene, N. Chniba Boudjada, W. Boujelben, Ceram. Int. **44**, 12723 (2018)
9. A. Urushibara, Y. Moritomo, T. Arima, A. Asamitsu, G. Kido, Y. Tokura, Phys. Rev. B **51**, 14103 (1995)
10. D. Grossin, J.G. Noudem, Solid State Sci. **6**, 939 (2004)
11. J. Moradi, M.E. Ghazi, M.H. Ehsani, P. Kameli, J. Solid State Chem. **215**, 1 (2014)
12. A. Elghoul, A. Krichene, N. Chniba Boudjada, W. Boujelben, Ceram. Int. **44**, 14510 (2018)
13. S. Fearn, J.C.H. Rossiny, J.A. Kilner, J.R.G. Evans, Solid State Ion. **211**, 51 (2012)
14. S.M. Salili, A. Ataie, M.R. Barati, Z. Sadighi, Mater. Charact. **106**, 78 (2015)
15. M. Zarifi, P. Kameli, M.H. Ehsani, H. Ahmadvand, H. Salamati, J. Supercond. Nov. Magn. **10948**, 4066 (2017)
16. Z.X. Wei, S.B. Ye, X.M. Wang, Ceram. Int. **42**, 9196 (2016)
17. R.D. Shannon, Acta Crystallogr. A **32**, 751 (1976)
18. A. Krichene, W. Boujelben, A. Cheikhrouhou, J. Alloy. Compd. **581**, 352 (2013)
19. A. Krichene, R. Thaljaoui, W. Boujelben, J. Supercond. Nov. Magn. **28**, 1881 (2016)
20. A. Krichene, P.S. Solanki, S. Rayaprol, V. Ganesan, W. Boujelben, D.G. Kuberkar, Ceram. Int. **41**, 2637 (2015)
21. R. Li, Z. Qu, J. Fang, X. Yu, L. Zhang, Y. Zhang, Solid State Commun. **150**, 389 (2010)
22. R. Li, Z. Qu, J. Fang, Physica B **406**, 1312 (2011)
23. A. Krichene, M. Bourouina, D. Venkateshwarlu, P.S. Solanki, S. Rayaprol, V. Ganesan, W. Boujelben, D.G. Kuberkar, J. Magn. Magn. Mater. **408**, 116 (2016)
24. A. Krichene, W. Boujelben, S. Mukherjee, N.A. Shah, P.S. Solanki, Ceram. Int. **45**, 3849 (2019)
25. R.R. Zhang, G.L. Kuang, B.C. Zhao, Y.P. Sun, Solid State Commun. **150**, 209 (2010)
26. J.L. García-Muñoz, C. Frontera, M.A.G. Aranda, C. Ritter, A. Llobet, L. Ranno, M. Respaud, J. Vanacken, J.M. Broto, J. Magn. Magn. Mater. **242–245**, 645 (2002)
27. Z.C. Xia, L.X. Xiao, C.H. Fang, G. Liu, B. Dong, D.W. Liu, L. Chen, L. Liu, S. Liu, D. Doyananda, C.Q. Tang, S.L. Yuan, J. Magn. Magn. Mater. **297**, 1 (2006)
28. J.L. García-Muñoz, C. Frontera, M.A.G. Aranda, A. Llobet, C. Ritter, Phys. Rev. B **63**, 064415 (2001)
29. V.K. Pecharsky, K.A. Gschneidner Jr., J. Magn. Magn. Mater. **200**, 44 (1999)
30. V. Franco, A. Conde, Int. J. Refrig. **33**, 465 (2010)